

# CHICKEN HEART DISEASE CHARACTERIZATION BY MULTI-SPECTRAL IMAGING

K. Chao, Y.-R. Chen, W. R. Hruschka, B. Park

**ABSTRACT.** *Optical spectral reflectance and multi-spectral image analysis techniques were investigated to characterize chicken hearts for real-time disease detection. Spectral signatures of five categories of chicken hearts (airsacculitis, ascites, normal, cadaver, and septicemia) were obtained from optical reflectance measurements taken with a visible/near-infrared spectroscopic system in the range 473 to 974 nm. Multivariate statistical analysis was applied to select the most significant wavelengths from the chicken heart reflectance spectra. By optimizing the selection of wavelengths of interest for different poultry diseases, four wavelengths were selected (495, 535, 585, and 605 nm). The multi-spectral imaging system utilizes four narrow-band filters to provide four spectrally discrete images on a single CCD focal-plane. Using the filters at the wavelengths selected from the reflectance spectra, it was possible to easily implement multi-spectral arithmetic operations for disease detection. Based on analysis (t-test) of spectral image data, the multi-spectral imaging method could potentially differentiate individual diseases in chicken hearts in real time. All conditions except cadaver were shown to be separable (92–100%) by discriminant algorithms involving differences of average image intensities.*

**Keywords.** *Chicken heart disease, Food safety, Machine vision, Near-infrared reflectance, Spectral imaging, Spectroscopy.*

Inspection of poultry viscera is one of the tasks currently performed by human inspectors at poultry slaughter plants on each carcass for visual discrepancies resulting from diseases. Because of the significance of poultry viscera in the whole inspection process, full automation of poultry inspection awaits the development of techniques that can effectively identify individually contaminated conditions of poultry viscera. Studies on the development of methods for automated inspection of poultry viscera have focused on morphological measurements of internal organs. Using UV light to segregate spleen from other internal organs, Tao et al. (1998) used spleen enlargement measurements to classify wholesome and unwholesome poultry carcasses. For classification of poultry diseases from chicken liver and heart images, Chao et al., (1999) reported that RGB color information could be effectively used for differentiating normal livers from airsacculitis and cadaver livers. However, the RGB color images of chicken hearts could not be effectively used for the separation of diseased poultry carcasses.

This study was an attempt to use narrow band (rather than broadband RGB) images of chicken hearts for the separation of diseased poultry carcasses. High-resolution images, rather than simple spectrographic data, were gathered to give more flexibility in applications, such as generating size and

morphological information or detecting more localized conditions.

Diffusely reflected light contains information about the absorbers near the surface of a material. Spectral imaging involves measuring the intensity of diffusely reflected light from a surface at one or more wavelengths with relatively narrow band-passes. The resulting data for each sample is thus three-dimensional (two spatial dimensions and one spectral dimension). Because of the potentially large size of these data sets, spectral imaging often involves three stages: measuring spectra of whole samples at many wavelengths, selection of optimal wavelengths, and collection of images at selected wavelengths (Favier et al., 1998; Muir, 1993). In the first stage, the spatial dimensions are minimized or eliminated, and in the third, the wavelength dimension is restricted to a few wavelengths.

We chose a visible/near-infrared spectrophotometer to measure the spectra because of its previous success in providing useful information about chicken carcasses (Chen and Massie, 1993; Chen et al., 1996). From a set of relatively continuous spectra, it is possible to characterize spectral features with potential to separate different disease categories.

Several methods of wavelength selection are reported (Chen and Massie, 1993; Saputra et al., 1992). These involve some combination of visual inspection of the spectra, prior knowledge of spectral characteristics, and mathematical selection based on spectral difference or statistical correlation of reflection with diseased state. In this study we use discriminant analysis on a subset of the available wavelengths.

A multi-wavelength image collection system could be implemented in several ways: using a filter wheel, a liquid crystal tunable filter (LCTF), several cameras with filters, and single camera with beamsplitter. A critical issue that should be considered in real-time (at least 35 birds per minute) operations of these devices is the amount of time between sequentially acquired images at different wave-

---

Article was submitted in October 1999; reviewed and approved for publication by the Information & Electrical Technologies Division of ASAE in September 2000. Mention of company or trade names is for description only and does not imply endorsement by the U.S. Department of Agriculture.

The authors are **Kuanglin Chao**, ASAE Member, Agricultural Engineer, **Yud-Ren Chen**, ASAE Member Engineer, Research Leader, **William R. Hruschka**, Mathematician, USDA/ARS/ISL, Beltsville, Md.; and **Bosoon Park**, ASAE Member Engineer, Agricultural Engineer, USDA/ARS/PPMR, Athens, Ga. **Corresponding author:** Kuanglin Chao, USDA, ARS, ISL, Bldg. 303, BARC-East, 10300 Baltimore Avenue, Beltsville, MD 20705-2350; phone: (301) 504-8450; fax: (301) 504-9466; e-mail: chaok@ba.ars.usda.gov.

lengths. This is a function of both the image capture speed and the band switch speed. Electromechanical filter wheels are limited in the speed of wavelength switching. Improvement in LCTF technology makes a LCTF system superior to electromechanical filter wheels in both speed and flexibility of spectral selection (Evans et al., 1997). The time required for the LCTF to switch into a next wavelength is approximately 50 ms (Mao and Heitschmidt, 1998). However, this still makes the system unsuitable for synchronizing with moving objects at high-speed inspection. Recent advances in optical design make the four-band imager, based on stationary filters and a beamsplitter, promising for real-time operation. It has the advantage of no moving parts and the simultaneous capture of images at four different wavelengths with good image registration. Such a system was used for this work.

The objectives of this study were (1) to determine the optimal wavelengths for a multi-spectral imaging system; (2) to discriminate individual chicken heart types; and (3) to identify features from multi-spectral images that can be effectively used for characterizing condemned conditions of chicken hearts.

## MATERIALS AND METHODS

### CHICKEN HEART SAMPLES

Hearts were taken from chicken carcasses identified as belonging to one of five inspection categories: airsacculitis, ascites, normal, cadaver, and septicemia. Airsacculitis is commonly used to describe a respiratory syndrome in broiler chicken. The hearts from airsacculitis carcasses have a fibrinous coating firmly attached. Ascites is characterized by accumulation of fluid or exudate within the body cavity.

Cadaver is caused by improper slaughter cuts or inadequate bleeding time. Septicemia is a system disease caused by pathogenic microorganisms in the blood.

These samples were identified and collected by a USDA Food Safety and Inspection Service (FSIS) veterinarian from a poultry processing plant located on Maryland's Eastern Shore. Samples were marked according to the condemnation conditions and placed in plastic bags to minimize dehydration. Then the bags were placed in coolers, filled with ice, and transported to the Instrumentation and Sensing Laboratory (within 2 h) for the experiments.

### EXPERIMENTAL SYSTEMS

**Diode-Array Spectroscopic System.** The experimental system used to measure the spectra of poultry hearts is built around a photodiode array spectrophotometer system. The schematic of the system is depicted in figure 1. This system consisted of a tungsten-halogen light source with power supply, fiber-optic probe, photodiode array detector, spectrograph, and personal computer.

Light emitted from a 100 W quartz tungsten halogen lamp travels through a bifurcated fiber optic cable (Fostec ModelC03267, Auburn, N.Y.) and exits at a concentric ring of optical fibers. The emitted light interacts with the chicken heart and the diffusely reflected light is collected through a 5 mm diameter aperture in the center of the concentric optical probe. The sample holder is a white Teflon cylinder with inside dimensions 5 cm high and 5 cm diameter. The walls and base of the cylinder are 1.5 cm thick. Hearts are roughly elliptically shaped with major and minor axes approximately 4 cm and 2.5 cm. A sample is placed in the bottom of the cylinder. The probe is mounted in a white

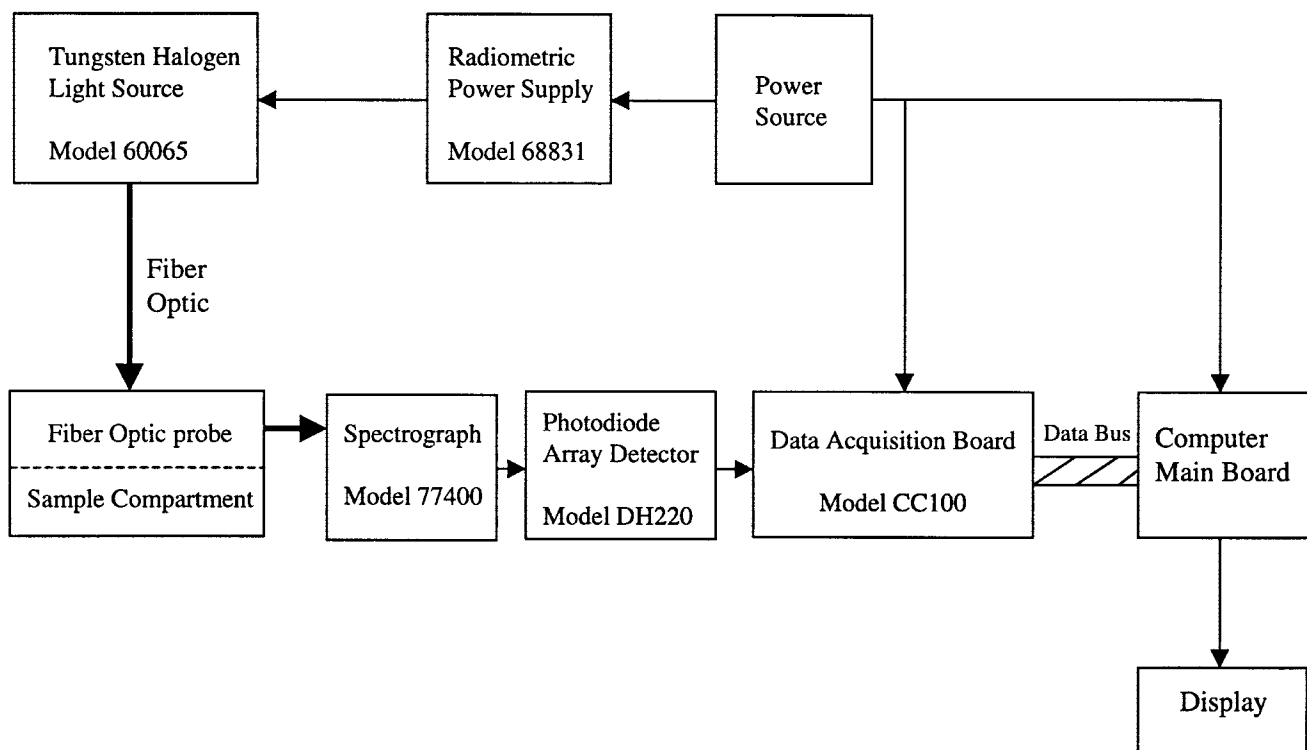


Figure 1. Layout of the photodiode array spectrophotometer system.

Teflon cylinder cover 1.5 cm thick, so that the distance from the probe to the sample is 2 cm. This arrangement serves to amplify the signal, because light diffusely reflected from the sample can reenter the sample after interacting with the Teflon, resulting in more absorbance before finally reentering the collecting fiber bundle. Teflon is chosen because it is highly scattering while having low and flat absorbance.

The collected light travels back through the bifurcated fiber bundle to a spectrograph (Model 77400, Oriel, Stratford, Conn.) which is attached to a silicon photodiode array detector (1024 diodes) (Model DH220, Oriel, Stratford, Conn.). The spectrograph has a focal length of 120 mm and a ruled grating (400 lines/mm). The photodiode array detector is connected to a computer (Pentium MMX 200 MHz) via an interface card (Model CC100, Oriel, Stratford, Conn.). This interface card provides a 16-bit analog-to-digital converter that converts the analog signal from each diode and transfers the data to the computer.

**Multi-Spectral Imaging System.** A multi-spectral imaging system (Figure 2a) was assembled to capture four-spectral images on a single focal plane. The system consists of an illumination chamber ( $0.46 \times 0.61 \times 0.43$  m high) with four halogen lamps, monochrome CCD detector, spectrometer with four interference filters, frame grabber, and personal computer.

Four 20 W DC halogen lamps (Philips Lighting Co., Somerset, N.J.) were used as the light source to provide 2460 lux (lumen/m<sup>2</sup>) light on the chicken heart surface. One lamp was mounted on each of the top four corners of the chamber about 0.3 m from the sample at an angle of 45° from the vertical. The reflected light from the sample was passed through a 17-mm focal length lens (Schneider Inc., Kreuznach, Germany) which was attached to the spectrometer. The spectrometer (MultiSpec Patho-Imager™, Optical Insights, LLC, Tucson, Arizona) consists of a set of proprietary optics designed to separate an object into spectrally discrete images on a single detector focal plane. Figure 2b illustrates the optical layout of the spectrometer. The light transmitted through the objective lens is passed through a field stop. Then the light is collimated and re-transmitted to a four-side reflected beam-splitter, which splits the light path directly to the four mirrors. The angle of each mirror is adjustable so that the reflected light can be emitted from individual interference filters to the CCD detector (Model TM-9701, PULNIX Inc., Sunnyvale, Calif.) to form a multi-band signal on a single focal plane. The CCD detector converts the four-band signal to an electrical signal that is amplified by the CCD preamplifier and sent to an image capture board (Model PX610, Imagenation Corp., Beaverton, Oreg.) which is installed in a PCI expansion slot of the computer.

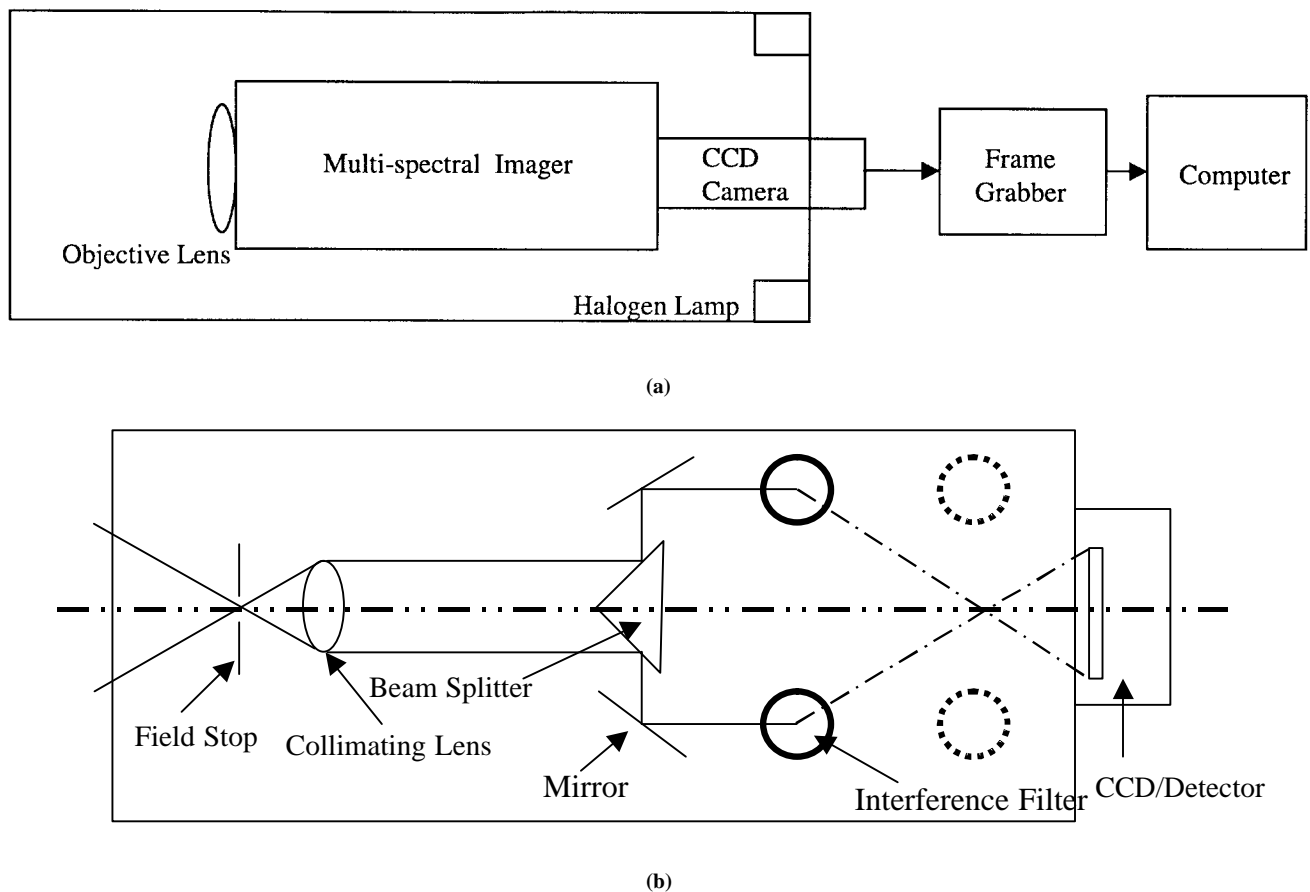


Figure 2. Layout of the multi-spectral imaging system: (a) overall system block diagram; (b) optical diagram for the multi-spectral imager.

## PROCEDURES

### Visible/Near-Infrared Reflection Measurement.

Spectral data were collected using the diode-array spectroscopic system. The system was wavelength-calibrated using a high intensity mercury lamp before each spectral measurement session. The spectral emission of the mercury lamp was measured at three different wavelengths (546.69, 577.10, and 579.06 nm). A white reference measurement was taken using a white Teflon block placed against the probe receptor with the light source on for total energy output from the light source. A dark reference was taken with the light source off to compensate for the zero energy signals. Spectra were recorded as percent according to the formula

$$\% \text{ Reflectance} = 100 \times (\text{sample reflectance} - \text{dark reference}) / (\text{white reference} - \text{dark reference}).$$

Each spectrum was measured by an average of 244 scans (32.8 ms/scan, 8 s exposure). A total of 40 poultry hearts (8 in each category) collected in November 1998 were used for the spectral measurements, one spectrum of each heart.

The slit/grating/array arrangement provided an approximate sampling interval of 0.5 nm between diode elements in the range 473 to 974 nm, with a band-pass of approximately 0.4 nm. The wavelength reproducibility is better than 0.01 nm, as shown by the repeated measurement of the mercury lines before each experimental session. The three decimal place numbers used below are for computation purposes only. Each spectrum had 1024 data points from 472.625 nm to 974.374 nm spaced 0.491 nm apart. Each spectrum was smoothed with a Savitzky-Golay (Hruschka, 1987) quadratic polynomial fitting 21 adjacent points (to simulate a ~10 nm band-pass). The spectrum was then interpolated quadratically, and reduced to 98 points (480 to 965 nm at 5 nm intervals).

The spectra and accompanying classification were then used in a SAS 6.12 (SAS Institute Inc., Cary, N.C.) stepwise selection procedure (PROC STEPDISC), followed by a linear discrimination (DISCRIM) using the wavelengths selected by the stepwise procedure. This was done to find an optimal subset of wavelengths that could separate the five categories.

**Multi-Spectral Imaging Measurement.** A total of 125 chicken hearts (25 in each category), collected in March and April 1999, were used for this part of the experiment. Multi-spectral images were measured using four interference filters selected from the optimal wavelength set found in the visible/near-infrared reflection experiment. For each wavelength selected the filter had a 20 nm band-pass. Four images, one per filter, were imaged on a single detector focal plane for each chicken heart sample. The 8-bit image was digitized by the image capture board with 640 (horizontal)  $\times$  480 (vertical) pixel resolution, so that the image corresponding to one filter was approximately 320  $\times$  240 pixels. A typical set of four sub-images is shown in figure 3.

Image processing sequences including image enhancement, image alignment, and identification of features of interest were applied to analyze the multi-spectral images. The image analysis uses the brightness of regions in the

image as a means of identification. It assumed that the same type of feature would have the same brightness whenever it appears in the field of view. However, the image obtained from the multi-band system shows vignetting, in which the corners of the image are darker than the center (Figure 3). To alleviate this effect, a background image of a uniform reference surface (optical grade black acrylic) was applied as a template to level the subsequent images. The image enhancement procedure was performed by dividing the acquired image by the background template.

Since the sub-images acquired from the four-band system are not perfectly aligned, image registration is needed before image differencing could be applied to generate an image database from the multi-spectral images. Manual registration involving shifting pixels on the x-y direction was performed with the aid of a commercially available software program (Melange™, Optical Insights, LLC, Tucson, Ariz.). Figure 4 shows the program operation. Mouse-controlled row and column offsets are performed until registration is visually satisfactory.

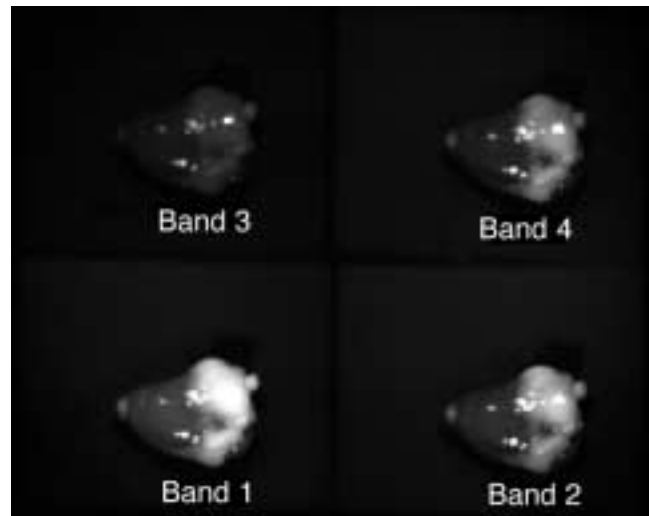
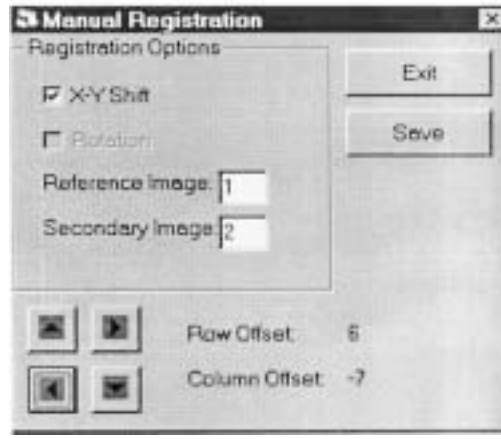
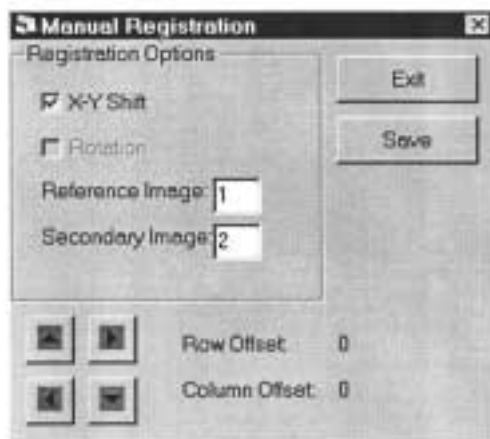
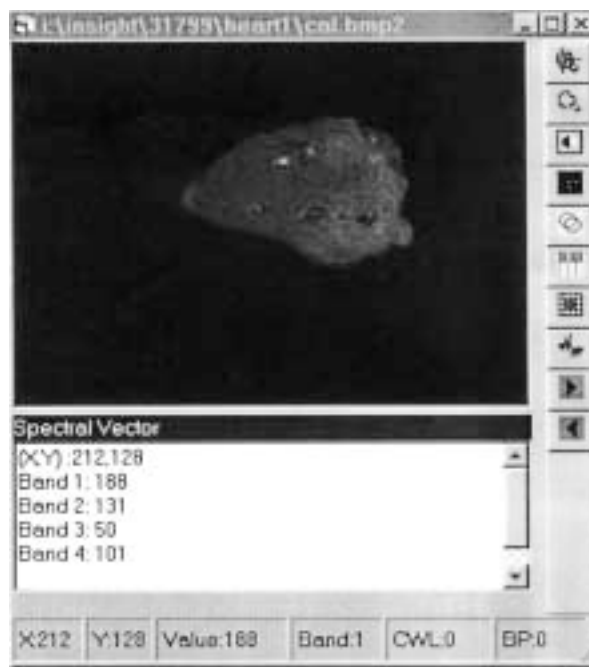


Figure 3. Four-band spectral images for a normal chicken heart.

The final step in the image processing was to use a dynamic thresholding process to set all pixels not of the heart or connected tissue to zero. From then on, only the non-zero pixels in each image were considered.

Ten processed images were extracted for each chicken heart: the original four background-corrected and registered images, and six difference images created from these as follows: The average image intensities obtained from filters 1 to 4 were ordered descending (band 1, band 2, band 4, and band 3). Then, six difference images (bands 1 - 2, 1 - 3, 1 - 4, 2 - 3, 2 - 4, and 4 - 3) were created. A total of 1250 images 320 pixels wide  $\times$  240 pixels high were generated. The average gray-level intensities for the ten processed images of each chicken heart were calculated by dividing the sum of the reflectance intensities of the non-zero image pixels by the number of non-zero pixels.



(a)

(b)

Figure 4. Image alignment: (a) before pixel shift operation; (b) after pixel shift operation.

## RESULTS AND DISCUSSION

### REFLECTANCE SPECTRA OF CHICKEN HEARTS

Figure 5 depicts the average reflectance spectra for the five different chicken heart categories. These results indicate that over the spectrum (473 to 974 nm), the most distinctive difference among the five chicken heart types occurred in the region from 475 to 600 nm. The absorption bands at 520 and 560 nm could be an indication of oxymyoglobin or oxyhemoglobin absorption, while the absorption at 740 nm could be a combination of fat, water, deoxymyoglobin, and deoxyhemoglobin absorptions. The spectral features of these two absorption areas might form a major base for the wavelength selection to differentiate normal chicken hearts from the abnormal chicken hearts. The overall vertical offset of a particular spectrum is caused by variable scatter and surface reflectance effects, and small changes in distance to the sample, which have little to do with the category characteristics. To reduce the visual impact of this effect,

each average spectrum was offset so that each had an adjusted value of 25 at 680 nm (Figure 6). These normalized results are less sample-dependent. Thus, it is clearly indicated that the spectrum region from 490 to 600 nm is the best for wavelength selection. This expectation was fulfilled in the DISCRIM wavelength selection process.

### SELECTION OF WAVELENGTHS

Table 1 summarizes the results of the individual steps in the stepwise procedure performed for wavelength selection. The significance level of 0.40 was set for entering variables into the discriminating set. The significance level of 0.15 was set for removing variables from the set. Seven wavelengths (495, 535, 550, 555, 585, 590, and 605 nm) were selected by the stepwise procedure. This selection corroborated the above visual indication that the 490 to 600 nm region would be the most useful for discrimination.

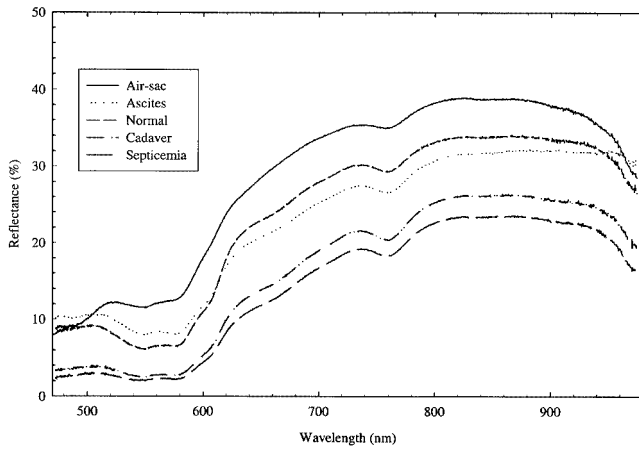


Figure 5. Comparison of the average reflectance as a function of wavelength for the chicken heart samples.

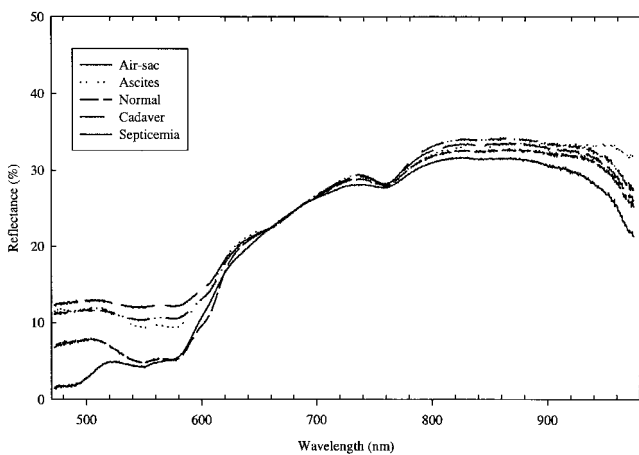


Figure 6. Comparison of the reflectance normalized with the intensity at 680 nm as a function of wavelength for the chicken heart samples.

The F statistic shown on the top of Table 1 is the largest F value obtained by performing a one-way analysis on each of the candidate wavelengths (98 points from 480 to 965 nm at 5 nm intervals). The wavelength at 535 nm is selected first, because it has the largest F value and is significant at the 0.40 level. At the beginning of step 2, the procedure checks to see if wavelength at 535 nm can be removed from the set of selected variables, and since this wavelength is significant at the 0.15 level, it is not removed. The procedure then looks for the next wavelength to be selected. The F statistics shown in the fifth column of Table 1 are the largest F values obtained by performing a one-way analysis of covariance on each of the remaining candidate variables using wavelength at 535 nm as the covariate. The stepwise process continues through the next several steps (3 to 7) resulting in selection of five more wavelengths 495 nm, 550 nm, 605 nm, 590 nm, and 555 nm.

Table 1. Summary of statistics for wavelength selection by stepwise selection procedure.

Stepwise Selection	Wavelength Entered (nm)	Wavelength Removed (nm)	One-way ANOVA F statistic	One-way ANCOVAR F statistic	Prob>F
Step 1	535	N/A	26.156		0.0001
Step 2	585	No		9.372	0.0001
Step 3	495	No		7.772	0.0002
Step 4	550	No		5.645	0.0015
Step 5	605	No		2.988	0.0339
Step 6	590	No		5.423	0.0021
Step 7	555	No		5.350	0.0024
Step 8	530	No		1.949	0.1702
Step 9		530			0.1702

Table 2. Confusion matrix for classification of chicken hearts using all 98 wavelengths and the four selected wavelengths (495, 535, 585, and 605 nm) (the four-wavelength results are in parentheses).

Actual	Predicted					Percentage
	Air-sac	Ascites	Normal	Cadaver	Septicemia	
Air-sac	<b>8 (8)</b>	0 (0)	0 (0)	0 (0)	0 (0)	100 (100)
Ascites	0 (1)	<b>8 (7)</b>	0 (0)	0 (0)	0 (0)	100 (88)
Normal	0 (0)	1 (1)	<b>7 (6)</b>	0 (1)	0 (0)	88 (75)
Cadaver	0 (0)	0 (0)	0 (1)	<b>3 (2)</b>	5 (5)	38 (25)
Septicemia	0 (0)	0 (0)	0 (0)	2 (2)	<b>6 (6)</b>	75 (75)

Of the seven wavelengths chosen by the DISCRIM procedure, four (495, 535, 585, and 605 nm) were chosen to use in the multi-spectral imaging system. These were not the first four chosen by the SAS program, but it was thought that because the filters were to have a 20 nm band-pass, selecting wavelengths without overlapping would maximize the information obtained by the camera. Table 2 shows the classification results using all 98 wavelengths and using the four chosen for multi-spectral imaging. Classification ability decreased only slightly when only 4 of the 98 wavelengths were used. Note also that more than 70% of cadaver samples were classified to septicemia hearts, which indicates that it is difficult to differentiate cadaver hearts from septicemia hearts.

#### MULTI-SPECTRAL IMAGING CHARACTERIZATION OF CHICKEN HEARTS

Table 3 summarizes significance t-test results for comparing mean reflectance intensity values from the normal, airsacculitis, ascites, cadaver, and septicemic chicken hearts at four different single-wavelength (495, 535, 585, 605 nm) and the six difference images. The mean reflectance intensities of the airsacculitic heart allowed separation from those of ascites, normal, septicemic, and cadaver hearts at all single-wavelength and difference images (excluding 585 to 495 nm). The mean intensities of the ascites hearts were also significantly different ( $P < 0.001$ ) from those of normal and septicemic hearts at all single-wavelength and difference images.

**Table 3. Significance test results for comparing mean reflectance intensity values from the normal, airsacculitis, ascites, cadaver, and septicemic chicken hearts at four single-wavelengths and their subtraction spectral images.**

Wave-length (nm)	Air-Asc	Air-Nor	Air-Sep	Air-Cad	Asc-Nor	Asc-Sep	Asc-Cad	Nor-Sep	Nor-Cad	Sep-Cad
605	8.6284*** (0.0000)	16.8604*** (0.0000)	32.6532*** (0.0000)	11.9088*** (0.0000)	5.2888*** (0.0000)	16.7998*** (0.0000)	3.5217** (0.0017)	12.2252*** (0.0000)	-1.0238 (0.3161)	-10.0078*** (0.0000)
585	8.9626*** (0.0000)	16.2311*** (0.0000)	23.5351*** (0.0000)	11.8239*** (0.0000)	5.6094*** (0.0000)	14.6079*** (0.0000)	4.4399*** (0.0001)	12.3937*** (0.0000)	0.5781 (0.5685)	-6.6696*** (0.0000)
535	3.4624** (0.0021)	9.9682*** (0.0000)	17.2460*** (0.0000)	10.6175*** (0.0000)	3.4700** (0.0019)	9.3958*** (0.0000)	4.7579*** (0.0000)	8.4522*** (0.0000)	1.9031 (0.0690)	-3.9301*** (0.0006)
495	2.3544* (0.0187)	4.7065*** (0.0000)	8.5412*** (0.0000)	4.1780*** (0.0003)	2.7177* (0.0120)	9.3128*** (0.0000)	2.1494* (0.0418)	9.5545*** (0.0000)	-0.5826 (0.5656)	-9.5468*** (0.0000)
605-585	-11.8503*** (0.0000)	3.5031*** (0.0001)	4.5680*** (0.0001)	-15.8102*** (0.0000)	21.3251*** (0.0000)	20.9684*** (0.0000)	-1.0789 (0.2913)	2.9393*** (0.0000)	-30.9192*** (0.0000)	-23.7831*** (0.0000)
605-535	17.8017*** (0.0000)	18.8855*** (0.0000)	45.3697*** (0.0000)	23.5751*** (0.0000)	4.7865*** (0.0000)	27.1859*** (0.0000)	0.1950 (0.8470)	19.9211*** (0.0000)	-3.19812** (0.0038)	-26.2525*** (0.0000)
605-495	3.2346** (0.0035)	9.5280*** (0.0000)	13.8529*** (0.0000)	2.8718** (0.0083)	7.9879*** (0.0000)	21.7208*** (0.0000)	-0.6576 (0.5170)	10.9161*** (0.0000)	-10.0174*** (0.0000)	-20.6305*** (0.0000)
585-535	21.9122*** (0.0000)	21.3653*** (0.0000)	32.0581*** (0.0000)	24.8658*** (0.0000)	-2.6466* (0.0141)	17.2000*** (0.0000)	-1.0572 (0.3009)	13.3664*** (0.0000)	1.6418 (0.1136)	-13.2730*** (0.0000)
585-495	7.3775*** (0.0000)	0.1587 (0.8752)	7.8544*** (0.0000)	0.4236*** (0.6756)	-10.3179*** (0.0000)	0.8711 (0.3923)	-10.2476*** (0.0000)	11.4503*** (0.0000)	0.3589 (0.7227)	-14.9201*** (0.0000)
535-495	8.8025*** (0.0000)	5.9275*** (0.0000)	28.2089*** (0.0000)	17.0077*** (0.0000)	-5.9711*** (0.0000)	10.1312*** (0.0000)	-0.0634 (0.9499)	32.0915*** (0.0000)	5.8453*** (0.0000)	-12.4493*** (0.0000)

Note: H<sub>0</sub>:  $\mu_1 = \mu_2$ ; H<sub>1</sub>:  $\mu_1 > \mu_2$ . ??Values in each column represent t-values and the asterisk (\*) means the significance levels.

\*P ≤ 0.05, \*\*P ≤ 0.01, \*\*\*P ≤ 0.001. Values in the parentheses are the P values for performing a significance test to reject null hypothesis ( $\mu_1 = \mu_2$ ).

Air = Aairsacculitis; Asc = Ascites; Nor = Normal; Sep = Septicemia; Cad = Cadaver.

However, no significant difference was found between ascites and cadaver hearts. Between normal and septicemic hearts, the mean reflectance intensities of normal were separable from the septicemic images by all single-wavelength and difference images. In case of comparison between normal and cadaver hearts, the spectral images from a single-wavelength were not useful. Instead, the difference images between 605 and 585 nm, between 605 and 495, and between 535 and 495 nm wavelength were significant (P < 0.001) for comparing two categories. For the comparison between septicemic and cadaver hearts, the mean intensities of all single-wavelength and difference images were significant (P < 0.001).

Table 4 shows the results from four single band (495, 535, 585, 605 nm) for classification of wholesome and unwholesome (airsacculitis, ascites, cadaver, and septicemia) chicken heart types. The results of the classification are presented in the form of a confusion matrix showing the numbers correctly classified (on the diagonal) and the numbers misclassified as another chicken heart types. Although the overall accuracy was low (66%), two of the categories showed high separability. The single-wavelength spectral images were useful for the identification of airsacculitis (92% correct) and septicemia (88%) chicken hearts from other chicken heart types. However, it was impossible to differentiate among ascites, cadaver, and normal using single-wavelength spectral images.

Although the single-wavelength spectral image has limited application for the classification, the difference images showed much better results (Table 5). Aairsacculitis, ascites, and septicemia showed near perfect separation, and normal did almost as well. Even the cadaver separation (84%) while not acceptable, showed some promise.

## SUMMARY AND CONCLUSIONS

This study was conducted to determine the feasibility of a novel multi-spectral imaging system for characterization of individual poultry disease from chicken hearts. In particular, the separability of five categories of hearts was studied (air sac, ascites, normal, cadaver, and septicemia).

Wavelengths were selected by stepwise discriminant analysis of visible/NIR spectral data. The visible wavelengths 495, 535, 585, and 605 nm were chosen from the seven significant wavelengths found by the discriminant analysis for use in the imaging system. The visible/NIR data at these wavelengths showed potential (at least 75% accuracy) for separating all categories except cadaver.

This potential was achieved by the multi-spectral imaging system. Gray-level image intensities at the four selected wavelengths and the six differences between intensities at pairs of wavelengths were used. The following conclusions were made using discriminant analysis:

1. With single-wavelength images, airsacculitis and septicemia were well separated (~90%).
2. With difference images, airsacculitis, ascites, normal, and septicemia were well separated (100%, 96%, 92%, and 100%, respectively).
3. Cadaver could not be separated as well, agreeing with the results from wavelength selection. However, the result (84%) is good enough to warrant research into more refined image processing algorithms.

This apparatus shows promise for real-time identification of poultry condemnation categories by automated image analysis of chicken hearts. Future research will involve automation of the image registration process and collection of samples under a variety of conditions, as well as

exploration of more complex statistical image characterization methods. With the increased use of automated viscera pack separation, this method should become an important part of any automated viscera inspection.

**Table 4. Confusion matrix for classification of chicken hearts using four single band images.**

Actual	Predicted					%
	Air-sac	Ascites	Normal	Cadaver	Septicemia	
Air-sac	<b>23</b>	2	0	0	0	92
Ascites	3	<b>12</b>	5	5	0	48
Normal	0	2	<b>15</b>	8	0	60
Cadaver	0	1	13	<b>11</b>	0	44
Septicemia	0	0	0	3	<b>22</b>	88

**Table 5. Confusion matrix for classification of chicken hearts using six difference images.**

Actual	Predicted					%
	Air-sac	Ascites	Normal	Cadaver	Septicemia	
Air-sac	<b>25</b>	0	0	0	0	100
Ascites	0	<b>24</b>	0	0	1	96
Normal	0	0	<b>23</b>	2	0	92
Cadaver	0	0	1	<b>21</b>	3	84
Septicemia	0	0	0	0	<b>25</b>	100

## REFERENCES

- Chao, K., Y. R. Chen, H. Early, and B. Park. 1999. Color image classification systems for poultry viscera inspection. *Appl. Eng. Agric.* 15(4): 363–369.
- Chen, Y. R., and D. R. Massie. 1993. Visible/near-infrared reflectance and interactance spectroscopy for detection of abnormal poultry carcasses. *Trans. ASAE* 36(3): 863–869.
- Chen, Y. R., R. W. Huffman, and B. Park. 1996. Changes in the visible/NIR spectra of chicken carcasses in storage. *J. Food Process. Eng.* 19(2): 121–134.
- Evans, M. D., C. N. Thai, and J. C. Grant. 1997. Computer control and calibration of a liquid crystal tunable filter for crop stress imaging. ASAE Paper No. 97–3141. St. Joseph, Mich.: ASAE.
- Favier, J., D. W. Ross, R. Tsheko, D. D. Kennedy, A. Y. Muir, and J. Fleming. 1998. Discrimination of weeds in brassica crops using optical spectral reflectance and leaf texture analysis. *SPIE* 3543: 311–318.
- Hruschka, W. R. 1987. Data analysis: wavelength selection methods. In *Near-Infrared Technology in Agricultural and Food Industries*, 35–55, ed. P. Williams and K. Norris. St. Paul, Minn.: American Association of Cereal Chemists.
- Saputra D., F. A. Payne, R. A. Lodder, and S. A. Shearer. 1992. Selection of near-infrared wavelengths for monitoring milk coagulation using principle component analysis. *Trans. ASAE* 35(5): 1597–1605.
- Mao C., and J. Heitschmidt. 1998. Hyperspectral imaging with liquid crystal tunable filter for biological and agricultural assessment. *SPIE* 3543: 172–181.
- Muir, A.Y. 1993. Machine vision and spectral imaging. *Agric. Eng.* 48(4): 124.
- Tao, Y., J. Shao, K. Skeeles, and Y. R. Chen. 1998. Detection of eviscerated poultry spleen enlargement by machine vision. *SPIE* 3544:138–145.